43rd Conference on
Our World in Concrete & Structures
30-31 August 2018, Singapore

PETROGRAPHIC OBSERVATION AND EVALUATION OF DEF IN CONCRETE USING FLY ASH CEMENT

Yoko Ando[*], Yuji Mitani[†], Takuya Ohno[‡], Joseph S.H. Lim[§] and Logendran Doraipandian[⊥]

[*]Taiheiyo Consultant Co., Ltd.
2-4-2 Osaku, Sakura, Chiba 285-0802, Japan
e-mail: <Youko_Andou@taiheiyo-c.co.jp> webpage: http://www.taicon.co.jp/

Keywords: DEF, fly ash cement, polarizing microscope, electron microscope, Duggan test, ettringite

Abstract. *The object of this study is to assess the risk of DEF in concrete made of fly ash cements. Optical and electron microscopic observation were performed. Concrete specimens were prepared assuming that they are used in mass concrete in the warm Southeast Asia regions including Singapore. Concrete specimens were mixed at room temperature 27°C, then exposed to maximum temperature 85°C assuming the interior of mass concrete. An accelerated DEF test was implemented in reference to Duggan test. After 3 cycles of heating and cooling, the specimens were submerged in water at 20°C. Expansion strain was measured and detailed petrographic observation was done. Concretes containing 30% fly ash (FA30) or 65% slag (BS65) produced no expansion in the Duggan test at 630 days. In polished thin sections, neither the formation of peripheral cracks around aggregates nor random cracks within cement paste was recognized. Electron microscopic observation showed that microcracks due to autogenous shrinkage in FA30 were less developed than in BS65. It was confirmed that FA30 produced better bonding around the aggregate. As an additional examination, ordinary portland cement was mixed with two levels of K_2SO_4 to elevate equivalent SO_3, then substituted by 30% fly ash. Concrete specimens at several SO_3 levels without fly ash produced extremely large expansion with remarkable cracks, i.e. peripheral cracks around aggregates, random cracks and ettringite within these cracks. By contrast, FA30 concretes produced no abnormal expansion. It was suggested fly ash was capable of suppressing DEF.*

1 INTRODUCTION

There are largely two types of expansion in concrete deterioration by sulfates: expansion caused by penetration of external sulfates; and expansion attributable to internal sulfates derived from cement. Delayed ettringite formation (DEF), which belongs to the latter type, has been known to

† Taiheiyo Singapore Pte. Ltd., Singapore
‡ Taiheiyo Cement Corporation, Japan
§ Island Concrete (Pte.) Ltd., Singapore
⊥ Singapore Cement Manufacturing Company (Pte.) Ltd., Singapore

occur mainly in precast concrete treated by high temperature steam curing. However, attention is being drawn to recent reports that point to concern of DEF risk in mass concrete[1,2].

Admixtures are considered to be effective in suppressing expansion by DEF. The DEF suppression effects of admixtures include dilution of sulfate ions in cement, reduction in pH of pore solution through consumption of OH^- during pozzolanic reaction, and, given sufficiently reactive Al_2O_3 contained in substituents, suppression of ettringite formation through precipitation of the sulfates as monosulfate[3]. It is also reported by a recent research[4] that a reduced Ca/Si ratio of CSH results in a reduced amount of leached Ca and thus a lower degree of ettringite supersaturation in the pore solution, leading to suppression of expansion. The reduction in Ca/Si ratio also results in an increased sorptivity of alkali[5] and a reduced concentration of the counterion, OH^-, likely contributing to the suppression of DEF through suppression of SO_4^{2-} release from the internal products. Another report says that alkali-fixation ability increases in CASH containing aluminum solid solution.

Concrete using ordinary portland cement (OPC) partially replaced with ground granulated blast furnace slag by more than 60% is widely used in Singapore as a means to suppress internal temperature rise in concrete members. However, slag concrete has large autogenous shrinkage strain, as well as large carbonation depth which requires increase in depth of concrete cover of reinforcement. In contrast to slag concrete, concrete using fly ash cement can have a reduced carbonation depth because a smaller amount of the admixture is adequate to reduce heat of hydration. Autogenous shrinkage strain is small, and pozzolanic reaction products densify the microstructure during the hydration process; which contributes to suppression of water transfer. One of the problems with fly ash concrete is significant variation in loss on ignition attributed to quality of fly ash which easily varies depending on the coal type, boiler type and burning temperature. This is considered to lead to a difficulty in controlling fresh concrete properties, especially the air content.

The purpose of this study is to evaluate the DEF suppression effect of fly ash cement using quality-managed low-Ca fly ash. An accelerated expansion test for DEF was carried out, and petrographic tests were performed by polarizing and electron microscopies. Assuming use for mass concrete structures in the warm Southeast region, fly ash concrete for the experiment was mixed in the environment of 27°C, and specimens were prepared by applying a temperature history to achieve the maximum temperature of about 85°C. The replacement ratio of fly ash in cement was 30%, with the balance between reduction in heat evolution and early strength development taken into account. Two methods are available for evaluation of DEF: LPC 66 test method by LCPC from France; and Duggan test method from the USA. By making reference to the method proposed by Duggan which used a more severe temperature history, the authors carried out expansion measurement by the accelerated DEF test and microscopic observation of the internal microstructure of the specimens to determine the DEF suppression effect of fly ash. In addition, the effect was examined in comparison with concrete containing 65% ground granulated blast furnace slag.

2 OUTLINE OF THE TESTS

2.1 Materials

OPC, fly ash (equivalent to Class C) and slag used in the experiment were all made in Japan. Tables 1 to 3 show the chemical compositions of the cement and admixtures, aggregates used and mix proportions of concrete, respectively. The water-binder ratio (W/(OPC+Alkali+FA+BS)) was 40% in all concrete mixes. The test mix was concrete using OPC partially replaced with fly ash by 30% (FA30), and the control mixes for comparative purposes were concrete using OPC partially replaced with slag by 65% (BS65) and concrete using plain OPC. Cements with increased risk of DEF were also prepared in two different levels by adding potassium sulfate to plain OPC to elevate equivalent SO_3 by 2% and 4%, respectively, and each of the high DEF risk cement was blended with 30% fly ash or 65% slag. Another two mixes with 2%-elevated SO_3 level were prepared to determine influence of alkali on DEF, by adding K_2SO_4 or $CaSO_4 \cdot 2H_2O$ (gypsum), respectively, to plain OPC.

Assuming use in the warm Southeast region including Singapore, concrete mixing was performed in the environment of 27°C, and cylindrical concrete specimens (diameter 100 mm, length 200 mm) were manufactured. After the concrete placement, the specimens were subjected to a temperature history simulating the condition inside the mass concrete to achieve the maximum temperature of about 85°C. Figure 1 shows the temperature history used. The accelerated

expansion test for DEF was carried out based on the method proposed by Duggan, applying three cycles of drying at 82°C and water curing at a room temperature to the specimens as shown in Figure 2.

The materials with the chemical compositions shown in Table 1 were used for FA30, BS65 and OPC+SO_3(2%), and those with similar properties coming from different lots were used for the other six mixes.

Table 1: Chemical compositions of cement and admixtures

Samples	Density	Specific surface area	Chemical composition and loss on ignition (mass%)												
	g/cm^3	cm^2/g	SiO_2	Al_2O_3	Fe_2O_3	CaO	MgO	SO_3	Na_2O	K_2O	TiO_2	P_2O_5	MnO	Cl	LOI
OPC	3.15	3320	20.65	5.66	2.93	63.1	2.5	2.07	0.21	0.38	0.29	0.21	0.08	0.020	1.70
FA	2.31	3810	55.77	26.63	5.03	3.1	1.16	0.36	0.73	0.91	1.59	0.45	0.07	0.000	3.41
GGBS	2.92	4480	32.73	13.53	0.3	43.9	5.14	2.10	0.22	0.27	0.48	<0.01	0.18	0.001	0.99

Table 2: Aggregates used

	Fine aggregates		Coarse aggregate
Symbols	S1	S2	G
Type	Crushed sand	Natural sand	Crushed granite
Source	Malaysia	Malaysia	Indonesia
Density (g/cm^3)	2.57	2.55	2.62

Table 3: Mix proportions of concretes

Specimens	W/B (%)	Unit contents (kg/m^3)							
		W	OPC	Alkali	FA	BS	S1	S2	G
FA30	40	165	289	0	124	0	398	286	1050
FA30+SO_3(2%)	40	165	277	13	124	0	398	286	1048
FA30+SO_3(4%)	40	165	264	25	124	0	397	285	1047
BS65	40	165	144	0	0	268	403	290	1063
BS65+SO_3(2%)	40	165	138	6	0	268	403	290	1063
BS65+SO_3(4%)	40	165	132	13	0	268	403	289	1062
OPC	40	165	413	0	0	0	408	293	1075
OPC+SO_3(2%)	40	165	395	18	0	0	407	293	1074
OPC+SO_3(2%Gyp)	40	165	395	18 (Gyp)	0	0	407	292	1072

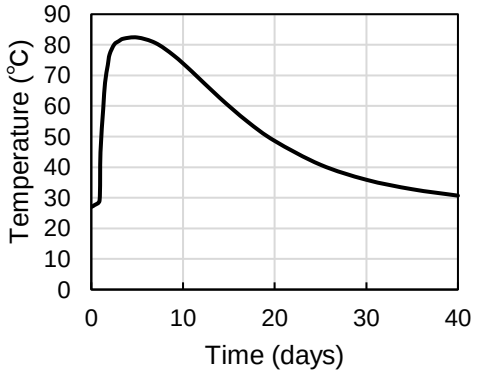

Figure 1: Temperature history simulating the condition inside the mass concrete

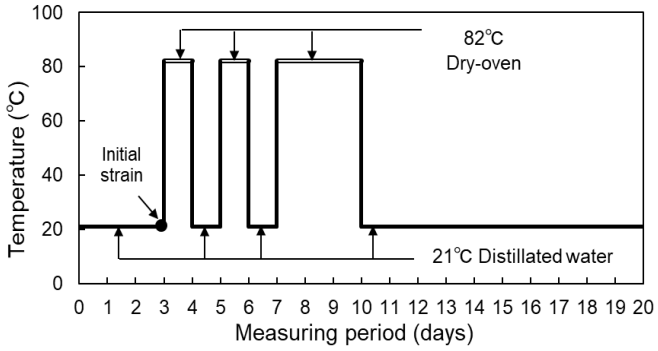

Figure 2: Curing conditions after the temperature history

2.2 Test methods

Expansion test

After applying three cycles of drying and rewetting as shown in Figure 2, expansion rate under 21°C water curing was determined. Measurement period was 630 days on FA30, BS65 and OPC+SO_3(2%), and 130 days on the other six mixes. Change in the length of each specimen was measured by the contact gauge method, using the ring gauges attached to the sides of the specimens. Calipers were used when the expansion rate exceeded the measurement range of the contact gauge.

Polarizing microscopy

Slices cut out of each specimen were strengthened by impregnation hardening using epoxy or fluorescent resin at ambient temperatures, and chips (2 cm × 3 cm) that include both aggregate particles and cement paste were cut out from the slices and polished into thin sections (15 to 20 μm thick) for polarizing microscopy.

Electron microscopy

The same polished thin sections after the polarizing microscopy were coated with carbon by vapor deposition, and microstructure observation was performed using backscattered electron images (BEI) by a scanning electron microscope (SEM). Quantitative analysis was made on major elements (SiO_2, TiO_2, Al_2O_3, Fe_2O_3, MnO, MgO, CaO, Na_2O, K_2O, SO_3 and P_2O_5) in the products detected under the electron microscope, using an energy dispersive X-ray spectrometer (EDS). XPP correction was applied to the analysis results.

3 RESULTS AND DISCUSSIONS

3.1 Expansion test

Figure 3 shows the accelerated expansion test results. No abnormal expansion was observed in FA30 and BS65 during the period of 630 days. Expansion of the plain OPC in 130 days was found to be below 0.1%. In contrast, OPC+SO_3(2%) to which alkali sulfate was added exhibited rapid expansion after about 50 days of water curing, reaching a rate of about 2.5% in 630 days with extremely large cracks occurring in the specimens. OPC+SO_3(2%Gyp) in which SO_3 level was elevated by adding gypsum also exhibited expansion of up to 0.5%. These suggest that DEF is likely to have occurred in OPC with SO_3 level elevated by 2%.

FA30+SO_3(2%), BS65+SO_3(2%), FA30+SO_3(4%) and BS65+SO_3(4%) were prepared by adding fly ash or slag to OPC+SO_3(2%) which exhibited abnormal expansion, or the cement with higher DEF risk whose SO_3 level was elevated by 4% by adding alkali sulfate to OPC. No abnormal expansion was observed in either of them during the 130-day period. The results showed that DEF was successfully suppressed in all of the concrete mixes using the high DEF risk cements partially replaced with 30% fly ash or 65% slag.

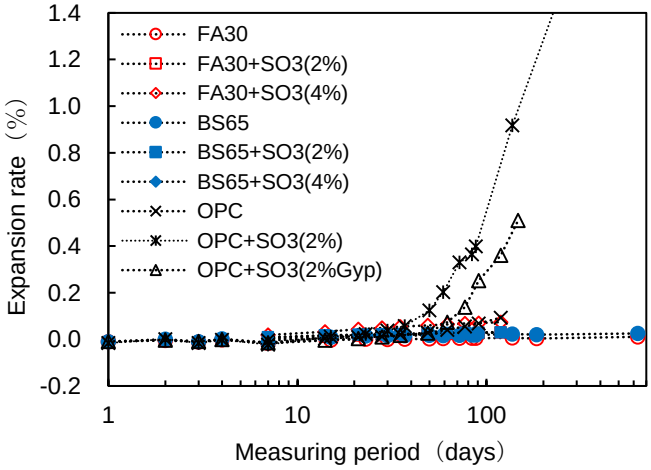

Figure 3: Expansion rate

Figure 4 shows the relationship between the molar ratio of SO_3/Al_2O_3 in cementitious material and the expansion rate of the specimens. Expansion occued in OPC+SO_3(2%) and OPC+SO_3(2%Gyp) where SO_3/Al_2O_3 was close to 1. The ratio was below 0.5 in other mixes with fly ash or slag admixture as well as in plain OPC, indicating no significant expansion. These results are in agreement with the report by Heinz and Ludwig (1987)[6] that there is a pessimum ratio of SO_3/Al_2O_3 in concrete for DEF-related expansion at around 1.0, and that DEF can be controlled at a ratio of 0.55 or below.

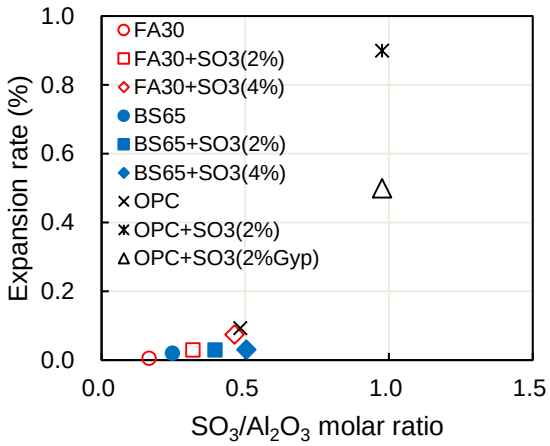

Figure 4: Molar ratio of SO_3/Al_2O_3 in cementitious material and expansion rate (after 140 days of water curing)

The major factors known to be associated with occurrence of DEF include temperature, water (humidity), sulfate ratio to aluminate phase in the cement, and alkali content in the concrete. According to Brown and Bothe (1993)[7], a high alkali content makes ettringite unstable and easily degradable during high-temperature curing, which promotes adsorption of SO_4^{2-} on CSH. The authors investigated the relationship between the presence/absence of added alkali and the amount of expansion. It was found that OPC+SO_3(2%) to which K_2SO_4 was added showed an increase in expansion after 30 days of water curing, while OPC+SO_3(2% Gyp) to which gypsum but no alkali was added to elevate SO_3 level showed an increase in expansion after 50 days. These suggest that 1) degradation of ettringite is accelerated under the high alkali conditions, making occurrence of DEF early and that 2) DEF occurs in the long term in the presence of SO_3 under the low alkali conditions.

3.2 Polarizing microscopy

Photos 1 to 2 show the polarized optical micrographs. FA30 and BS65 showed no gaps around the aggregate particles, network cracking in concrete or any other findings characteristic of DEF-affected concrete under the polarizing microscope. Similarly, no signs or evidence of DEF was found in the microstructure of FA30+SO_3(2%), BS65+SO_3(2%), FA30+SO_3(4%) and BS65+SO_3(4%) which were prepared by adding fly ash or slag to the high DEF risk cement.

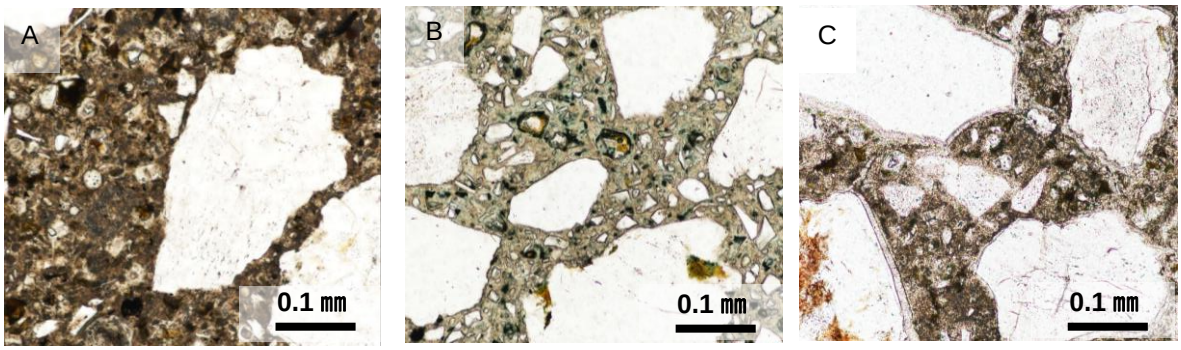

Photo. 1: Polarizing microscopy after 630 days of water curing
A, B: no microcracks around the aggregate surfaces and in the cement paste (A: FA30, B: BS65),
C: gaps around the aggregate surfaces, and cracks in the cement paste (OPC+SO_3(2%))

In contrast, OPC+SO_3(2%) and OPC+SO_3(2%Gyp) were found to have gaps around the aggregate particles and many microcracks in the cement paste microstructure, with needle crystals formed in the gaps and the cracks. In OPC+SO_3(2%) which was subjected to the 630-day expansion test, significantly wide gaps were formed around the coarse aggregate particles.

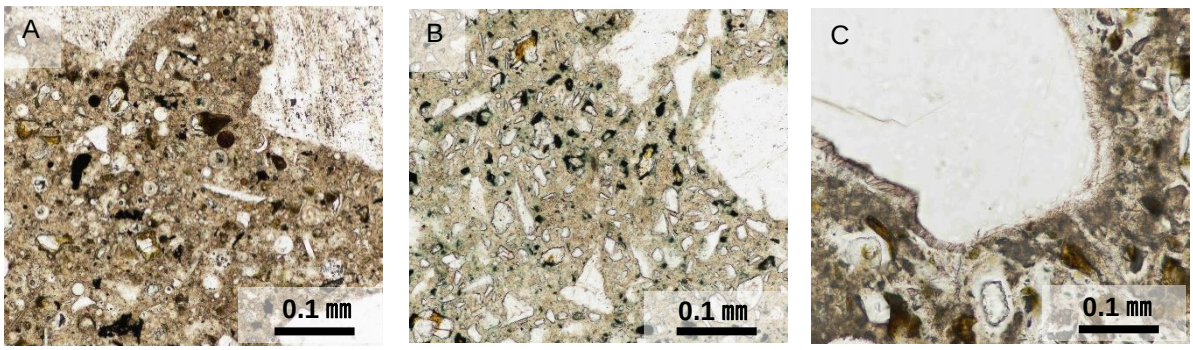

Photo 2: Polarizing microscopy after 130 days of water curing
A, B: no microcracks around the aggregate surfaces and in the cement paste（A: FA30+ SO_3(4%), B:BS65+ SO_3(4%)）, C: gaps around the aggregate surfaces, and cracks in the cement paste (OPC+SO_3(2%Gyp))

3.3 Electron microscopy

Photos 3 to 6 show BEI of the polished thin sections by SEM, and Table 4 shows the chemical compositions analyzed by EDS. No gaps around the aggregate particles or network cracking in the cement paste microstructure were found also by the SEM observation in FA30 (Photo 3) and BS65 (Photo 4) as well as in FA30+SO_3(2%), BS65+SO_3(2%), FA30+SO_3(4%) and BS65+SO_3(4%) which used the high DEF risk cement with fly ash or slag admixture. Of the products formed in FA30 or BS65 after the 630-day expansion test, which had no DEF-related expansion (Figure 3), ettringite was present only in a small amount contained in air voids or replacing cement hydrates without showing cracks or other evidence of deterioration. It was found that inner part of FA and slag remained left mostly unhydrated in FA30 and BS65 after the 630-day expansion test. On the other hand, ettringite was rare but monosulfate occurred replacing cement hydrates in FA30+SO_3(4%) and BS65+SO_3(4%) after the 130-day expansion test (Photo 5).

Both the microstructure observation results and the above accelerated expansion test results show that possibility of occurrence of DEF-related cracks would have been extremely low in all the mixes using OPC or the cement with 2%- or 4%-elevated SO_3 level partially replaced with 30% fly ash or 65% slag. Consequently, it was empirically confirmed that addition of fly ash or slag was effective in suppression of DEF.

In contrast, needle crystals were found in OPC+SO_3(2%) and OPC+SO_3(2%Gyp), filling the gaps in the cement paste-aggregate interfaces and the cracks in the cement paste (Photo 6). EDS quantitative analysis revealed that all of these needles were ettringite, showing occurrence of DEF. In OPC+SO_3(2%) which exhibited the largest expansion, ettringite needles were collectively formed in bundles, filling the gaps around the coarse aggregate particles or other significantly wide gaps, and individual needles were observed to grow separately.

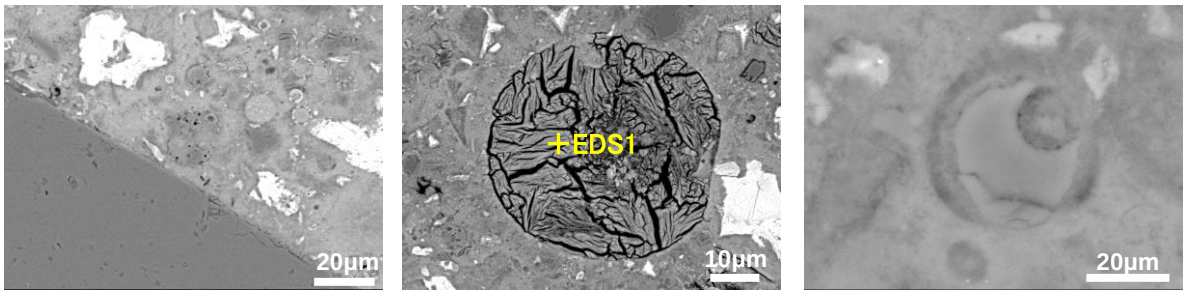

Photo 3: BEI of FA30 after 630 days of water curing
Bonding condition at the aggregate surfaces (left), ettringite formed in the void (middle), and reaction of FA (right)

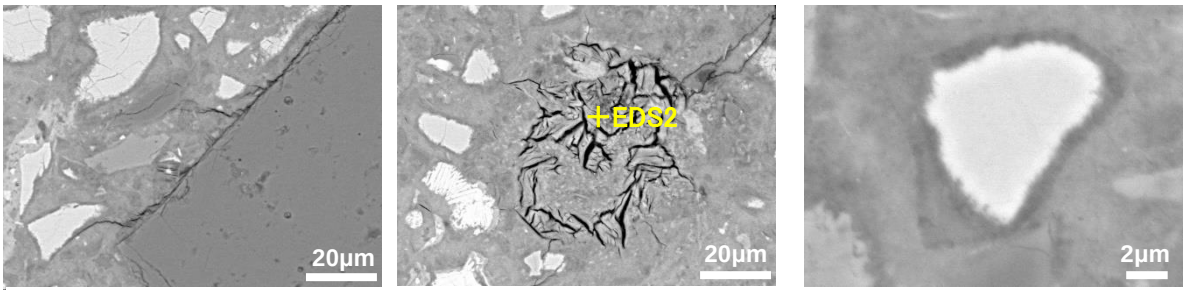

Photo 4: BEI of BS65 after 630 days of water curing
Bonding condition at the aggregate surfaces (left), ettringite formed in the void (middle), and reaction of slag (right)

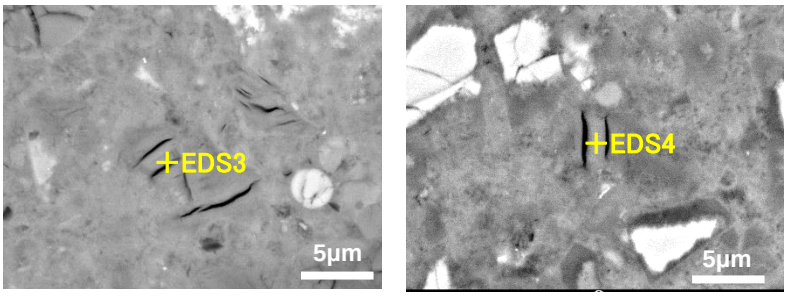

Photo 5: BEI of monosulfate in hydrates after 130 days of water curing
FA30+SO_3(4%) (left), BS65+SO_3(4%) (right)

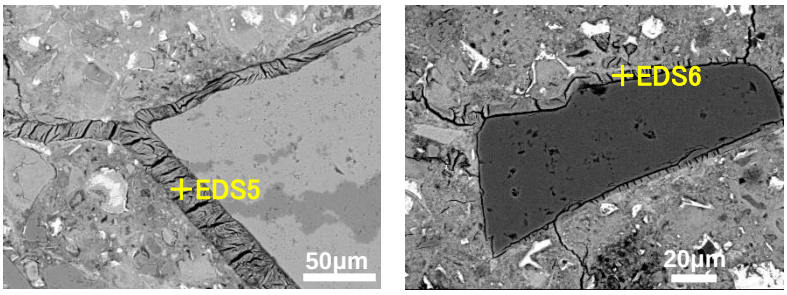

Photo 6: BEI of ettringite growing from the crystals formed in the gaps
OPC+SO_3(2%) after 630 days of water curing (left), OPC+SO_3(2%Gyp) after 130 days of water curing (right)

Table 4: EDS chemical composition analysis of hydrates in concrete (mass%)

Specimens	Locations	SiO_2	TiO_2	Al_2O_3	Fe_2O_3	MnO	MgO	CaO	Na_2O	K_2O	SO_3	P_2O_5	Total
FA30	EDS 1	1.49	0.02	12.63	0.39	0.11	0.04	35.11	0.10	0.05	27.33	0.00	77.27
BS65	EDS 2	1.68	0.10	11.96	0.00	0.00	0.01	35.04	0.00	0.09	27.80	0.06	76.74
FA30+SO_3(4%)	EDS 3	2.44	0.00	16.67	0.57	0.41	0.43	32.94	0.20	1.21	14.29	0.00	69.16
BS65+SO_3(4%)	EDS 4	1.34	0.00	14.66	0.39	0.00	0.31	35.97	0.04	0.34	11.94	0.81	65.86
OPC+SO_3(2%)	EDS 5	2.81	0.12	9.89	0.00	0.15	0.00	34.45	0.00	0.00	25.91	0.07	73.40
OPC+SO_3(2%Gyp)	EDS 6	3.81	0.03	10.46	0.00	0.32	0.01	36.06	0.14	0.02	25.77	0.00	76.69

Standardization as theoretical value of every mineral

1： Ettringite $(Ca_{5.32}, Mn_{0.01}, Mg_{0.01}, Na_{0.02}, K_{0.01})_{5.37}$ $(Al_{2.10}, Si_{0.21}, Fe_{0.04})_{2.36}$ O_6 $(SO_4)_{2.91}\cdot nH_2O$

2： Ettringite $(Ca_{5.43}, K_{0.01})_{5.44}$ $(Al_{2.04}, Si_{0.24}, Ti_{0.01})_{2.29}$ O_6 $(SO_4)_{3.03}\cdot nH_2O$

3： monosulfate $(Ca_{4.89}, Mn_{0.03}, Mg_{0.06}, Na_{0.02}, K_{0.15})_{3.69}$ $(Al_{1.91}, Si_{0.24}, Fe_{0.04})_{2.18}$ O_6 $(SO_4)_{1.04},\cdot nH_2O$

4： monosulfate $(Ca_{3.95}, Mg_{0.05}, Na_{0.01}, K_{0.04})_{4.05}$ $(Al_{1.77}, Si_{0.14}, Fe_{0.03})_{1.94}$ O_6 $(SO_4)_{0.92}\cdot nH_2O$

5： Ettringite $(Ca_{551}, Mn_{0.02})_{5.53}$ $(Al_{1.74}, Si_{0.42}, Ti_{0.01})_{2.17}$ O_6 $(SO_4)_{2.91}\cdot nH_2O$

6： Ettringite $(Ca_{5.33}, Mg_{0.04}, Na_{0.02})_{5.4}$ $(Al_{1.70}, Si_{0.53})_{2.23}$ O_6 $(SO_4)_{2.67}\cdot nH_2O$

Bonding condition at the aggregate surfaces in FA30 and BS65 after the 630-day expansion test was examined. In FA30 very good bonding condition was observed at the aggregate surfaces, with no DEF-related gaps formed around the aggregate surfaces. In contrast, BS65 was found to have partially poor bonding at the cement paste-aggregate interfaces and cracks developing along the peripheries of aggregate particles, though the bonding condition at the aggregate surfaces was generally good. There is a report by Mitani *et al.* (2016)[8] that autogenous shrinkage strain in BS65 is more than three times that in FA30. These suggest that the microcracks found around the aggregate particles in BS65 may have been caused partly due to the large autogenous shrinkage in BS65.

To examine alkali-fixation ability of hydrates containing aluminum in solid solution, Figures 5 and 6 show the diagrams Ca/Si-Ca/(Na+K) and Ca/(Si+Al)-Ca/(Na+K) in the systems FA30+SO_3(4%) and BS65+SO_3(4%) with added K_2SO_4, respectedly, with reference to method after Katayama (2012)[9]. EDS analysis was made at several points ranging from unhydrated part of fly ash, slag and alite to hydrates surrounding each. The results showed that alkali sorption by fly ash was more strongly correlated with Ca/(Si+Al) than with Ca/Si, indicating the effect of aluminum. The point of convergence exists where hydrate of admixture and hydrate of alite have identical chemical composiotion after the progress of hydration in an equilibrium state. Ca/(Si+Al) had a convergent point at 1.2 to 1.3 in both FA30+SO_3(4%) and BS65+SO_3(4%); in contrast, Ca/(Na+K) had a convergent point at 1.0 in FA30+SO_3(4%) but at around 10 in BS65+SO_3(4%). This indicates a very high alkali-fixation ability of fly ash hydrate with low Ca/(Si+Al) and Al has the same effect as Si in hydrates.

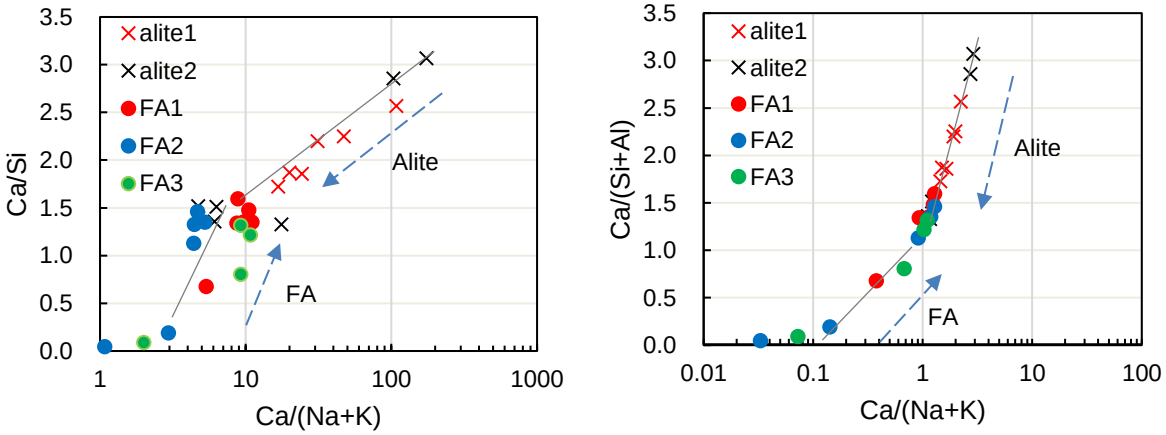

Figure 5: Hydration of alite and fly ash in FA30+SO_3(4%)
(after 130 days of water curing)

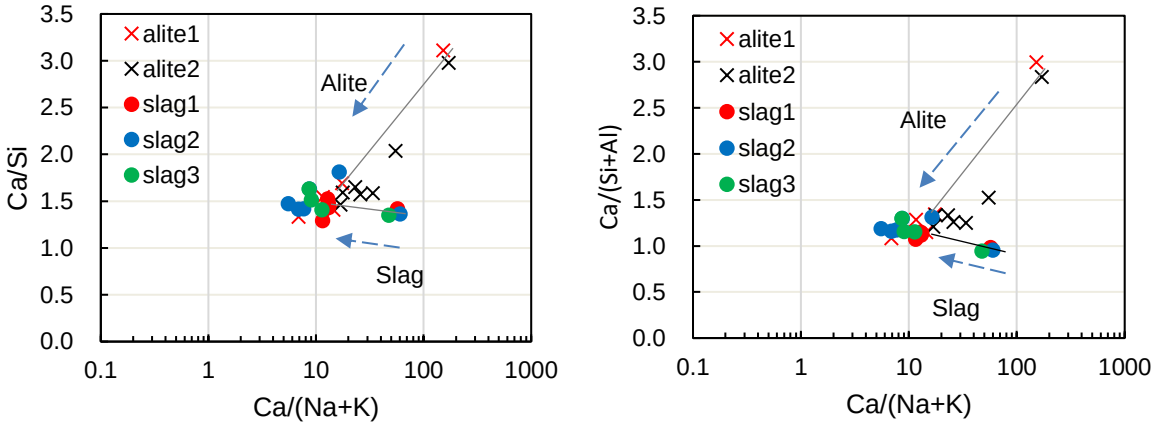

Figure 6: Hydration of alite and slag in BS65+SO_3(4%)
(after 130 days of water curing)

However, the chemical composition of hydrates could contain extremely fine ettringite or monosulfate undetectable by the electron microscopy. Figure 7 shows the analytical values of SO_3 and Al_2O_3 in hydrates contained in FA30+SO_3(4%) and BS65+SO_3(4%), respectively, plotted on the logarithmic axis. Chemical compositions of the CSH of plain OPC were included for comparative purposes, and composiotions of platy hydrates (AFm phase) in each specimen detectable by the electron microscopy are also plotted. The dotted lines in the graphs represent the ideal chemical compositions of ettringite (AFt) and monosulfate (AFm) converted to total anaritical values assuming the analysis in a vacuum (ettringite 72%, monosulfate 66%). It was found that hydrate around alite in FA30+SO_3(4%) had an intermediate chemical composition between those of ettringite and monosulfate, while hydrates around fly ash had a similar chemical composition to that of monosulfate. In contrast, both hydrates around alite and those around slag in BS65+SO_3(4%) were found to have similar chemical compositions to that of monosulfate.

The above observations suggest the following possibilities about SO_3 in FA30+SO_3(4%): 1) SO_3 is present in a solid solution of hydrates, 2) SO_3 is contained in minute inclusions of monosulfate or intermediate chemical compositions between ettringite and monosulfate, and 3) calcium silicate hydrates adsorb SO_4^{2-} ions.

In any case, the DEF suppression effect of fly ash is attributable to the high alkali-fixation ability of hydrates with low Ca/(Al+Si) which prevents release of counterions, i.e., OH^- and SO_4^{2-}, into the pore solution, as well as the enhanced OH^- consumption through pozzolanic reaction.

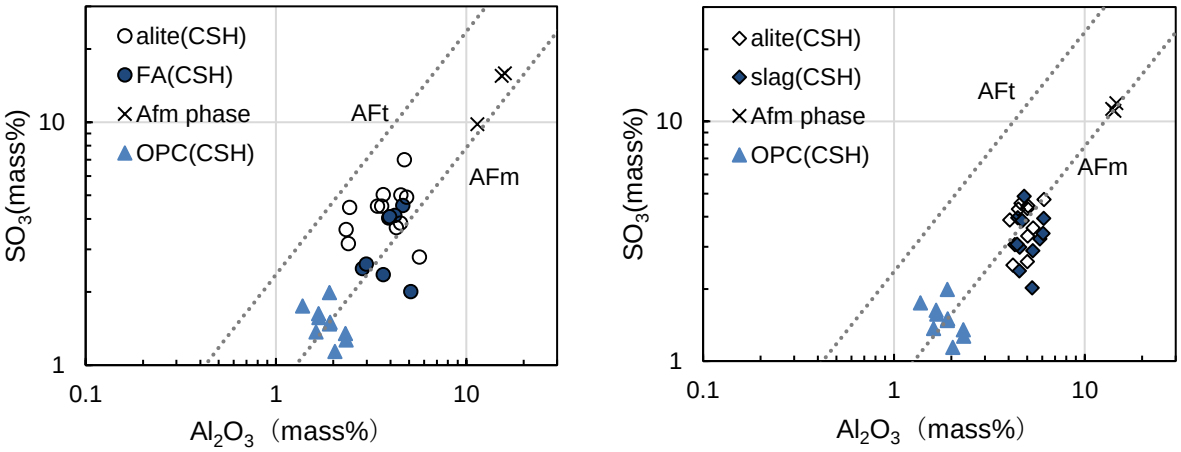

Figure 7: Relationship between Al_2O_3 and SO_3 in hydrates (after 130 days of water curing) FA30 +SO_3(4%)(left), BS65 +SO_3(4%)(right)

4 CONCLUSIONS

Risk of DEF and DEF suppression effect of fly ash were investigated by an accelerated expansion test and microscopic observation of the internal microstructure, using concrete specimens subjected to an early temperature history with the maximum temperature of about 85°C to simulate the condition inside the mass concrete. The major findings are summarized below:

(1) No abnormal expansion was observed during the accelerated test in blended OPC with 30% fly ash or 65% ground granulated blast furnace slag as well as in plain OPC. There were also no findings characteristic of DEF in their microstructures under the microscopes. DEF is not likely to have occurred in these specimens.

(2) Abnormal expansion was observed in the specimens using OPC with SO_3 level elevated by 2% by adding alkali sulfate or gypsum. Microscopic observation revealed the presences of gaps in the cement paste-aggregate interfaces, microcracks in the cement paste and ettringite filling them, confirming the occurrence of DEF. These indicate that, irrespective of the presence/absence of the alkali, increase in SO_3 content can cause DEF in the concrete exposed to high temperature history. On the other hand, within the range of this test, DEF occurred in the earlier stage in the alkali-added specimens as compared to the specimens without alkali addition.

(3) Alkali sulfate was added to OPC to prepare cements with SO_3 level elevated by 2% and 4%, respectively, and blended cements partially replaced with 30% fly ash or 65% slag

were prepared using each of them. No abnormal expansion was observed in either of them, and microscopic observation revealed no findings characteristic of DEF in their microstructures. These indicate that DEF in concrete using high DEF risk cements can be successfully suppressed by adding 30% fly ash or 65% slag for partial replacement.

(4) The concretes added with fly ash were found to have dense microstructure of cement paste and very good bonding at the aggregate surfaces. In addition, cracks developing along the peripheries of the aggregate surfaces were found less frequently in them as compared to those added with slag. The reason for this is likely the smaller autogenous shrinkage strain in the concretes using fly ash than that in high slag concretes.

(5) Correlation of alkali sorption in hydrate with Ca/(Si+Al) in the concrete mixes containing fly ash was stronger than that with Ca/Si, indicating the effect of aluminum.

ACKNOWLEDGEMENT

The authors would like to express their gratitude to Professor Kazuyuki Torii, Kanazawa University, and Dr. Shinichi Hirono, Taiheiyo Consultant Co., Ltd., for their guidance and also to Dr. Tetsuya Katayama, Taiheiyo Consultant Co., Ltd., for his advice in correlating analytical data and discussion in this study.

REFERENCES

[1] Japan Concrete Institute, The Guidelines for Control of Cracking of Mass Concrete 2016 (2016).

[2] B. Godart and L. Divet, *Lessons learned from structures damaged by delayed ettringite formation and the French prevention strategy*, 5th international conference on Forensic Engineering (2013).

[3] T. Ramlochan, M.D.A. Thomas and R.D. Hooton, *The effect of pozorrans and slag on the expansion of mortars cured at elevated temperature Part II: Microstructural and microchemical investigations,* Cement and Concrete Research 34 (2004) 1341-1356.

[4] W. Kunther, B. Lothenbach and J. Skibsted, *Influence of the Ca/Si ratio of the C-S-H phase on the interaction with sulfate ions and its impact on the ettringite crystallization pressure,* Cement and Concrete Research 69 (2015) 37-49.

[5] B. Lothenbach and A. Nonat, *Calcium silicate hydrates: Solid and liquid phase composition*, Cement and Concrete Research 78 (2015) 57-70.

[6] D. Heinz and U. Ludwig, *Mechanism of secondary ettringite formation in mortars and concretes subjected to heat treatment*, Concrete durability, SP-100, V. 2, American Concrete Institute (1987) 2059-2071.

[7] P.W. Brown and J.V. Bothe, *The stability of ettringite,* Advances in Cement Research, Vol. 5, No. 18 (1993) 47-63.

[8] Y. Mitani, T. Ohno and K. Toda, *Phisical properties and thermal cracking risk of concrete using fly ash cement under the southeast asia enviroment,* The 7th International Conference of Asian Concrete Federation (2016) 8p.

[9] T. Katayama, *ASR gels and their crystalline phases in concrete -- universal products in alkali-silica, alkali-silicate and alkali-carbonate reactions*, Proceedings, 14th International Conference on Alkali-Aggregate Reaction in Concrete (ICAAR), Austin, Texas, USA, paper 030411-KATA-03 (2012).